Generating characteristic acoustic impedances with hydrogel based phononic crystals for use in ultrasonic transducer matching layers

Paul Daly
Centre for Ultrasonic Engineering
University of Strathclyde
Glasgow, United Kingdom
paul.daly@strathclyde.ac.uk

Dr Joseph Jackson
Centre for Ultrasonic Engineering
University of Strathclyde
Glasgow, United Kingdom
joseph.jackson@strath.ac.uk

Prof James F. C. Windmill
Centre for Ultrasonic Engineering
University of Strathclyde
Glasgow, United Kingdom
james.windmill@strath.ac.uk

***Abstract*—The impedance matching layer has a critical effect on ultrasonic transducer performance, but it is difficult to source materials that have the appropriate acoustical properties. A method that utilises effective property relations of composites and finite element analysis is used to design a hydrogel-steel based phononic crystal, quarter wavelength impedance matching layer that can match bespoke configurations. Phononic crystal band structures are calculated to determine an appropriate lattice scale length, and frequency domain studies are carried out to compare this novel type of matching layer with an ideal bulk layer. Transmitted pressure curves are as expected and suggest that this design type will be suited for fabrication and testing.**

Keywords—ultrasonic transducer, impedance matching layer, phononic crystal, sonic crystal, hydrogel, finite element, model

I. Introduction

An acoustic impedance matching layer (IML) is often attached to the front face of a bulk wave ultrasonic transducer (UT) to mitigate the large impedance mismatch between the piezoelectric element and the target medium. The reduction of a mismatch enhances efficient energy transfer and consequently, UT and system performance [1]. They can often be the limiting component of an entire system [2]. Developments to the IML will benefit many ultrasonic applications (e.g. biomedical therapy and diagnosis, underwater sonar, non-destructive testing, structural condition monitoring, industrial processing and control, and materials characterization [3]).

There is a small selection of materials that can alleviate a UT-load mismatch and even those with a suitable impedance can be excessively attenuating, or unsuitable for mounting and deployment [1] [4] [5] [6] [7]. A cascade of intermediate IMLs increase the UT's bandwidth [8] [9] [10] [11] but multiple sections compound the problem of material scarcity and introduces the issue of joining with adhesives. The adhesives are layers themselves, and introduce inaccuracies, complexity in analysis, modelling and fabrication, and undesirable losses [5].

Consideration of these issues suggest that it would be beneficial if an IML, composed of a single continuous body, with a particular, tuned impedance, could be manufactured using common fabrication tools. Different methodologies that have attempted to satisfy these criteria have been available in the literature [1]. Recent publications have shown that a phononic crystal (PhC) can operate as an IML [12] [13] [14] [15].

Phononic and sonic crystals (SC) have been used to abate the propagation of waves, both vibrational [16] and acoustical [17], as well as for wave focusing [18], energy harvesting [19], frequency filtering [20], waveguiding [21], sound diffusion [22], liquid sensing [23] and as an acoustic diode [24].

In this work the aim is to fulfil the criteria given above and design a quarter-wavelength IML that simplifies or surpasses existing solutions and circumvents the typical problems [25] [26]. Simulations of a PhC with a hydrogel matrix and steel cylindrical scatterers is used to match PZT with a central operating frequency of 100 kHz to a water load. The method presented will allow for the tuning of properties to match bespoke UT-load configurations, and as additive manufacture become increasingly commonplace in the laboratory and workspace, one that end users can implement themselves.

II. Method

A. Effective properties

In 2007, Mei et al used Multiple Scattering Theory (MST) to derive expressions for the effective density and effective elasticity of fluid-solid and solid-solid composites composed of a matrix and scatterers in the long wavelength, or zero frequency, limit [27]. Their results that are pertinent to this work are summarised below.

In the following, subscripts a denotes the scattering inclusion and b the background matrix, and f is the filling fraction. A sonic crystal (SC) with a fluid matrix has effective density $\rho_{eff} = \rho_b \times (\rho_a (1+f) + \rho_b (1 - f)) / (\rho_a (1 - f) + \rho_b (1 + f))$ and effective bulk modulus $1 / K_{eff} = 1 / K_a + (1 - f) / K_b$.

A phononic crystal with a solid matrix has effective density $\rho_{eff} = \rho_a f + \rho_b (1 - f)$ and effective first and second Lamé parameters $\lambda_{eff} = (\lambda_b + \mu_b - \mu_{eff} + S (\mu_b + \mu_{eff})) / 1 - S$ (where $S = ((\lambda_a + \mu_a) f - (\lambda_b + \mu_b) f) / (\lambda_a + \mu_a - \mu_b)$ is a simplifying term) and $\mu_{eff} = \mu_b \times ((\mu_a + \mu_b) + (\mu_a - \mu_b) f) / ((\mu_a + \mu_b) - (\mu_a - \mu_b) f)$.

When the scatterers are highly concentrated and have impedances considerably greater than the matrix, wave scattering effects and the wave path's increased tortuosity reduce the wave speed relative to that of the matrix. The effective acoustic wave speed in an SC is $c_{eff} = (K_{eff} / \rho_{eff})^{1/2}$ and effective longitudinal and transverse wave speeds (for P- and S-waves) in a PhC are $c_{L,eff} = ((\lambda_{eff} + 2\mu_{eff}) / \rho_{eff})^{1/2}$ and $c_{T,eff} = (\mu_{eff} / \rho_{eff})^{1/2}$. (Note that Mei et al use the relation $M = \lambda + \mu$ for the P-wave modulus whereas here $M = \lambda + 2\mu$ [12] [28]).

This is a peer reviewed, accepted author manuscript of the following research article:
Daly, P., Jackson, J., & Windmill, J. F. C. (2021). Generating characteristic acoustic impedances with hydrogel based phononic crystals for use in ultrasonic transducer matching layers. In 2021 IEEE International Ultrasonics Symposium (IUS) (pp. 1-4). (IEEE International Ultrasonics Symposium, IUS). IEEE. https://doi.org/10.1109/IUS52206.2021.9593874

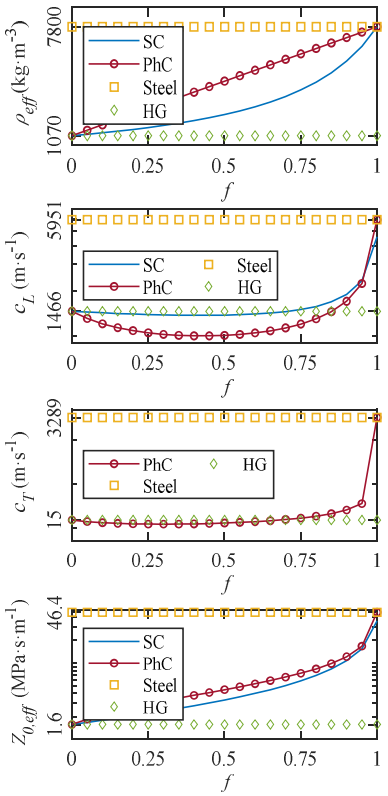

Fig.1 The effect of filling fraction on (First) effective mass density, (Second) longitudinal wave speed, (Third) transverse wave speed and (Fourth) characteristic specific acoustic impedance is presented. The solid lines and solid lines with circular markers are for sonic and phononic crystals. Static values for steel and a hydrogel are shown using square and diamond markers. Note that (First) only has a linear scale.

The effect of f on these properties, as well as effective characteristic specific acoustic impedance $Z_{0,eff} = \rho_{eff}\, c_{L,eff}$, are presented in Fig.1 using mass densities and Lamé parameter values for a hydrogel matrix and steel scatterers. These values are, respectively, ρ_{hg} = 1070 kg m^{-3}, λ_{hg} = 2.3 GPa, and μ_{hg} = 0.24 MPa, and ρ_s = 7800 kg m^{-3}, λ_s = 107.4 GPa, and μ_s = 84.4 GPa [12]. Here, a hydrogel is also considered as a fluid. First, to compare PhC and SC expressions and second, because the water content of a hydrogel can become very high. To do so, the bulk modulus is expressed as $K = \lambda + 2\mu / 3$ [28].

The impedances of the PZT transducer and water load are Z_{PZT} = 33.50 MPa s m^{-1} and Z_w = 1.48 MPa s m^{-1}, respectively. For a quarter-wavelength IML, $Z_{ML} = (Z_{PZT}\, Z_w)^{1/2}$ = 7.0 MPa s m^{-1} [1]. The filling fraction that generates the desired Z_{ML} value, and consequently effective density and wave speed, is calculated. For a PhC these values are 0.73, 5.99 × 10^3 kg m^{-3} and 1.18 × 10 m s^{-1}, and for a SC 0.81, 4.43 × 10^3 kg m^{-3} and 1.59 × 10 m s^{-1}.

The ratio of cylindrical scatterer r to lattice constant a is extracted from the definition of f in square and hexagonal lattices— $f_{sqr} = \pi r^2 / a^2$ and $f_{hex} = 2\pi r^2 / \sqrt{3} a^2$. For a PhC these quotients r / a equal 0.48 and 0.45, and for a SC 0.51 and 0.47, respectively.

B. *Band structure*

The ω-k band structure of a crystal can be calculated [29] (or measured [30]) and inspected to ensure that the UT central operating frequency does not lie within any of the crystal's bandgaps, and to determine the onset of the long wavelength regime. Only in this regime are the effective property relations valid (because, to a wave with sufficiently large wavelength, the crystal appears homogenous).

Here, the commercial FEM package COMSOL Multiphysics is used to carry out a 2D Frequency Domain, Eigenfrequency simulation of a unit cell [31]. The method is detailed by COMSOL but is described here in brief [32]. Floquet periodicity is applied to each pair of parallel faces on the unit cell boundary (which, in effect, transforms a cell into one of an infinite array that behaves identically). The components [k_x, k_y] of a parameter k are varied and the wavevector follows the perimeter of the Irreducible Brillouin Zone (IBZ) (the points ΓXMΓ and ΓKMΓ in the square and hexagonal reciprocal lattices). The eigenfrequencies of the system are calculated at each point in the k-path and plotted as a function of k to generate the band structure.

The Bragg condition of destructive interference is satisfied when the distance between scatterers $\Delta x = \pi / k$, where $c = \omega / k$ [33]. Accordingly, in a phononic crystal, the lattice constant $a \approx 2\pi c_{eff} / \omega$. Shown in Fig.2 are the dispersion curves for a square lattice with a = 10 mm and f = 0.5, and for a hexagonal lattice with a = 5 mm and f = 0.75. A dotted line shows the central operating frequency of 100 kHz. Reducing a increases both the frequency at which the bandgap opens, and the extent of the long wavelength regime (i.e. where the first mode has a mainly linear gradient). An arbitrary reduction of a will cause manufacturing difficulties so it is suggested that a be on the scale of 1-2 mm.

In all FEA studies here the hydrogel is considered as a fluid with $c_{L,hg} = ((\lambda_{hg} + \mu_{hg}) / \rho_{hg})^{1/2}$ = 1.47 × 10^3 m s^{-1}. This is justified because of its high water content and because studies of a similar nature (i.e. the interaction between viscous fluids and solid structures) are often ill defined and prone to spurious solutions.

C. *Pressure wave propagation*

With f and a known (or its upper and lower limits) the efficacy of a PhC is validated using FEA in COMSOL.

The PhC sits between PZT and water, both of which are terminated by Perfectly Matched Layers. The PZT and water columns have heights 38.58 mm and 15 mm (corresponding to one wavelength at the central frequency), and a = 1.4 mm and r = 0.62 mm in the PhC. The PhC has a hexagonal lattice, and 4 and 11 vertical and horizontal layers. Consequently, the PhC is 5.0 mm deep and the whole assembly is 7.0 mm wide.

Floquet periodicity is applied to the vertical boundaries of all domains, which, in effect, means only an internal section of the whole UT-IML-water structure is considered. The k_x and k_y components of the Floquet wavevector vary with study frequency (although k_x = 0 as only normal incidence is considered).

The mechanical parameters of steel and hydrogel are as before (and again, the latter is treated as a fluid). The mass density, Young's modulus and Poisson's ratio of PZT are 7900 kg m^{-3}, 58.9 GPa, and 0.424. The mass denity and speed of sound of water are 1000 kg m^{-3} and 1500 m s^{-1}.

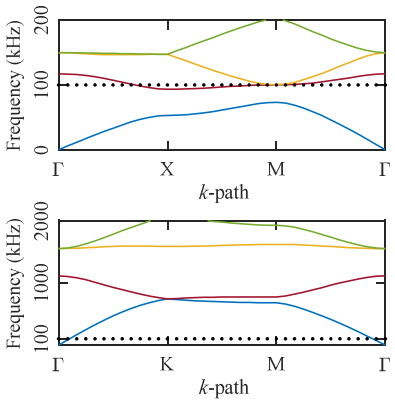

Fig.2 Band structures calculated using finite element analysis for a hydrogel-steel phononic crystal. The first figure is for a square lattice with a = 10 mm and f = 0.5, and second for a hexagonal lattice with a = 5 mm and f = 0.75. A dotted line is shown at 100 kHz.

To mimic the response of a UT, the PZT is split into two equal layers and the dividing line is excited with a velocity function, with $v_x = 0$ m s^{-1} and $v_y = 1\times10^8$ m s^{-1}, and oscillations are generated that propagate through the PhC into water. The resultant in water pressure is averaged.

Finally, the PhC is replaced by a fluid bulk mass, that is 7.2 mm deep and has mass density and sound speed equal to 2500 kg m^{-3} and 2902.8 m s^{-1}. Their product is one permutation of an ideal matching impedance.

III. Results

A comparison of the two pressure spectra generated using FEA in COMSOL is presented in Fig.3. Inspection shows that both types of IMLs maximise in water pressure at the expected frequency, and that the PhC is an effective medium in the long wavelength regime and is comparable to an ideal IML.

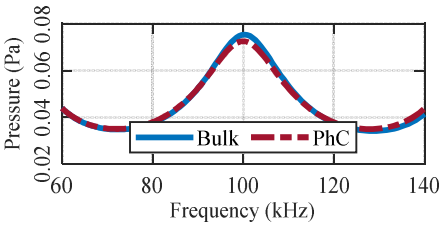

Fig.3 A comparison of averaged in water pressure for a bulk quarter wavelength impedance matching layer with ideal properties and a hydrogel-steel phononic crystal.

IV. Discussion

Both spectra have a near canonical profile and clearly have maxima centred over the operating frequency, as desired. It has been shown clearly that a PhC can function as a finely tuned, quarter wavelength IML. However, the models here are reliant on simplifications, and these ideal transmission curves are likely to change as these are replaced with more physically realistic features.

The first is the Floquet periodicity conditions: while this may represent an internal section of the structure well, physical boundaries are a necessity and will affect the response of all media. Certainly, by the way of reflections and potentially by excitation of structural modes which could generate resonant and anti-resonant features.

Second, is the lack of damping or thermoviscous effects in the model. All physical materials dissipate energy and so these features must be included in a realistic model. This is particularly relevant here where the primary purpose is to enhance energy transfer.

In the immediate future, these simplifications will be removed, and the effect of different length scales on the PhC IML's capabilities will be investigated. It will be compared against different materials that are used in practice. A more realistic simulation of a piezoelectric UT will be included in the model. Later, analytical tools (e.g. the Plane Wave Expansion method, MST and Finite Difference Time Difference method) will be incorporated into the design process.

Following more accurate modelling, the IML PhC will be fabricated and tested. The loss factor of both the hydrogel and the PhC can then be measured and included in FEA and improve the model's accuracy. The validity of the hydrogel fluid assumption can also be tested.

V. Conclusion

The impedance matching layer has a critical effect on ultrasonic transducer performance and sometimes can be the limiting component of an entire system. It is difficult to source materials that have the appropriate acoustical properties and are suitable for deployment.

Here, a method that utilises effective property relations of composites and finite element analysis has been proposed that will allow an end user to design a hydrogel-steel based phononic crystal impedance matching layer for bespoke configurations.

The method circumvents standard phononic crystal analytical tools, which require a significant time investment to implement. As phononic crystals are simple to fabricate (relative to some other impedance matching designs) it is believed that this design type will be successful in operation.

References

[1] V. T. Rathod, "A Review of Acoustic Impedance Matching Techniques for Piezoelectric Sensors and Transducers," Sensors, vol. 20, no. 14, p. 4051, 2020.

[2] G. Hayward, "The influence of pulser parameters on the transmission response of piezoelectric transducers," Ultrasonics, vol. 23, no. 3, pp. 103-112, 1985.

[3] A. Mulholland, N. Ramadas, R. O'Leary, A. Parr, G. Hayward, A. Trogé and R. Pethrick, "Enhancing the performance of piezoelectric ultrasound transducers by the use of multiple matching layers," IMA Journal of Applied Mathematics, vol. 73, pp. 936-949, 2008.

[4] T. E. G. Álvarez-Arenas, "Acoustic impedance matching of piezoelectric transducers to the air," IEEE Transactions on Ultrasonics, Ferroelectrics, and Frequency Control, vol. 51, no. 5, pp. 624-633, 2004.

[5] T. E. G. Álvarez-Arenas and L. Díez, "Novel impedance matching materials and strategies for air-coupled piezoelectric transducers," in SENSORS, 2013 IEEE, 2013.

[6] S. P. Kelly, G. Hayward and T. E. G. Álvarez-Arenas, "Characterization and assessment of an integrated matching layer for air-coupled ultrasonic applications," IEEE Transactions on Ultrasonics, Ferroelectrics, and Frequency Control, vol. 51, no. 10, pp. 1314-1323, 2004.

[7] L. Amoroso, S. N. Ramadas, C. Klieber, T. E. G. Álvarez-Arenas and T. McNally, "Novel Nanocomposite Materials for Improving Passive Layers in Air-coupled Ultrasonic Transducer Applications," in 2019 IEEE International Ultrasonics Symposium (IUS), 2019.

[8] S. T. Lau, H. Li, K. S. Wong, Q. F. Zhou, D. Zhou, Y. C. Li, H. S. Luo, K. K. Shung and J. Y. Dai, "Multiple matching scheme for broadband 0.72Pb(Mg1/3Nb2/3)O3−0.28PbTiO3 single crystal phased-array transducer," Journal of Applied Physics, vol. 105, p. 094908, 2009.

[9] J. H. Goll and B. A. Auld, "Multilayer Impedance Matching Schemes for Broadbanding of Water Loaded Piezoelectric Transducers and High Q Electric Resonators," IEEE Transactions on Sonics and Ultrasonics, vol. 22, no. 1, pp. 52-53, 1975.

[10] T. Manh, A.-T. T. Nguyen, T. F. Johansen and L. Hoff, "Microfabrication of stacks of acoustic matching layers for 15 MHz ultrasonic transducers," Ultrasonics, vol. 54, no. 2, pp. 614-620, 2014.

[11] M. I. Haller and B. T. Khuri-Yakub, "Tapered acoustic matching layers," in 1993 Proceedings IEEE Ultrasonics Symposium, 1993.

[12] E. Dong, Z. Song, Y. Zhang, S. G. Mosanenzadeh, Q. He, X. Zhao and N. Fang, "Bioinspired metagel with broadband tunable impedance matching," Science Advances , vol. 6, no. 44, pp. 1-9, 2020.

[13] K. Zhang, C. Ma, S. Lin, Y. Chen, Y. Zhang, N. X. Fang and X. Zhao, "Metagel with Broadband Tunable Acoustic Properties Over Air–Water–Solid Ranges," Advanced Functional Materials, vol. 29, no. 38, p. 1903699, 2019.

[14] E. Dong, Y. Zhang, Z. Song, T. Zhang, C. Cai and N. X. Fang, "Physical modeling and validation of porpoises' directional emission via hybrid metamaterials," National Science Review, vol. 6, no. 5, pp. 921-928, 2019.

[15] Y. Zhang, X. Gao, S. Zhang, W. Cao, L. Tang, D. Wang and Y. Li, "A biomimetic projector with high subwavelength directivity based on dolphin biosonar," Applied Physics Letters, vol. 105, no. 12, p. 123502, 2014.

[16] D. Richards and D. J. Pines, "Passive reduction of gear mesh vibration using a periodic drive shaft," Journal of Sound and Vibration, vol. 264, no. 2, pp. 317-342, 2003.

[17] J. V. Sanchez-Perez, C. Rubio, R. Martinez-Sala, R. Sanchez-Grandia and V. Gomez , "Acoustic barriers based on periodic arrays of scatterers," Applied Physics Letters, vol. 81, no. 5240-5242, 2002.

[18] A. Sukhovich, B. Merheb, K. Muralidharan, J. O. Vasseur, Y. Pennec, P. A. Deymier and J. H. Page, "Experimental and Theoretical Evidence for Subwavelength Imaging in Phononic Crystals," Physical Review Letters, vol. 102, no. 15, p. 154301, 2009.

[19] T.-G. Lee, S.-H. Jo, H. M. Seung, S.-W. Kim, E.-J. Kim, B. D. Youn, S. Nahm and M. Kim, "Enhanced energy transfer and conversion for high performance phononic crystal-assisted elastic wave energy harvesting," Nano Energy, vol. 78, p. 105226, 2020.

[20] J. N. Munday, C. B. Bennett and W. M. Robertson, "Band gaps and defect modes in periodically structured waveguides," The Journal of the Acoustical Society of America, vol. 112, pp. 1353-1358, 2002.

[21] A. Khelif, A. Choujaa, B. Djafari-Rouhani, M. Wilm, S. Ballandras and V. Laude, "Trapping and guiding of acoustic waves by defect modes in a full-band-gap ultrasonic crystal," Phys. Rev. B, vol. 68, no. 21, p. 214301, 2003.

[22] J. Redondo, V. Sánchez-Morcillo, Víctor and R. Picó, "The Potential for Phononic Sound Diffusers," Building Acoustics, vol. 18, no. 1-2, pp. 37-46, 2011.

[23] R. Lucklum and J. Li, "Phononic crystals for liquid sensor applications," Measurement Science and Technology, vol. 20, no. 12, p. 124014, 2009.

[24] X.-F. Li, X. Ni, L. Feng, M.-H. Lu, C. He and Y.-F. Chen, "Tunable unidirectional sound propagation through a sonic-crystal-based acoustic diode," Physical Review Letters, vol. 106, no. 8, 2011.

[25] J. Mei, Z. Liu, W. Wen and P. Sheng, "Effective dynamic mass density of composites," Physical Review B, vol. 76, no. 13, p. 134205, 2007.

[26] J. H. Goll, "The Design of Broad-Band Fluid-Loaded Ultrasonic Transducers," IEEE Transactions on Sonics and Ultrasonics, vol. 26, no. 6, pp. 385-393, 1979.

[27] J. Mei, Z. Liu, W. Wen and P. Sheng, "Effective dynamic mass density of composites," Physical Review B, vol. 76, no. 13, p. 134205, 2007.

[28] S. L. Garrett, Understanding Acoustics, Cham, Switzerland: Springer Nature, 2020, p. 187.

[29] J. Mei, Z. Liu, J. Shi and D. Tian, "Theory for elastic wave scattering by a two-dimensional periodical array of cylinders: An ideal approach for band-structure calculations," Phys. Rev. B, vol. 67, no. 24, p. 245107, 2003.

[30] C. Rubio, D. Caballero, J. V. Sanchez-Perez, R. Martinez-Sala, R. Sanchez-Grandia, J. Sanchez-Dehesa, F. Meseguer and F. Cervera, "The existence of full gaps and deaf bands in two-dimensional sonic crystals," Journal of Lightwave Technology, vol. 17, no. 11, pp. 2202-2207, 1999.

[31] COMSOL Multiphysics® v. 5.6., www.comsol.com, Stockholm, Sweden: COMSOL AB.

[32] N. Elabbasi, "Modeling Phononic Band Gap Materials and Structures," COMSOL AB, [Online]. Available: https://www.comsol.com/blogs/modeling-phononic-band-gap-materials-and-structures/. [Accessed 20 August 2021].

[33] A. Gupta, "A review on sonic crystal, its applications and numerical analysis techniques," Acoustical Physics, vol. 60, no. 2, pp. 223-234, 2014.